INFLUENCE OF LANTHANUM DOPING ON THE STRUCTURAL, MORPHOLOGICAL AND THERMAL CHARACTERISTICS OF NICKEL FERRITE

TRAIAN FLORIN MARINCA, MARIUS CRISTIAN OLARU,
BOGDAN VIOREL NEAMȚU, FLORIN POPA, IONEL CHICINAȘ

Abstract. Lanthanum doped nickel ferrite – $NiFe_{1-\delta}La_{\delta}O_4$ has been synthesised by solid state reaction using nickel and iron oxides (NiO and Fe_2O_3) and lanthanum hydroxide ($La(OH)_3$). The samples have been investigated by X-ray diffraction, in situ-high temperature X-ray diffraction, scanning electron microscopy, energy dispersive X-ray microanalysis, and differential scanning calorimetry. The amount of the lanthanum cations which enter in the cubic spinel structure is less than 1 % – related to 100 % of the one atom of Ni from the chemical formula of nickel ferrite – $NiFe_2O_4$. In the case of all doped samples that have been prepared a secondary phase with orthorhombic structure is resulting after the heat treatment: $LaFeO_3$ – orthoferrite. Upon increasing the lanthanum amount in the starting samples, the amount of the orthoferrite increases also. The secondary phase follows the contour of the lanthanum doped ferrite grains.

Key words: nickel ferrite, lanthanum doping, spinel ferrite, magnetic material, lanthanum orthoferrite.

1. INTRODUCTION

Nowadays the soft magnetic cubic spinel ferrites are used in wide applications in the electronics and electrics industries. Among the applications of the spinel ferrite can be mention multilayer chip inductor applications, deflection rings, filters, antennas, computer memory chips, recording heads, microwave devices, transducers, transformers, radio frequency, transformer cores, sensors [1–7]. The spinel ferrites are chemically stable, possess high electrical resistivity, low eddy current losses, moderate saturation magnetization and low costs. The Curie temperature of the soft magnetic ferrites is high [8–10]. Their chemical formula can be written as $MeFe_2O_4$, in which Me can be a metal or a group of metals with a total valence of 2+. Soft magnetic ferrites crystallize in the complex cubic spinel structure. This crystalline structure allows two types of sites for the metallic cations: tetrahedral

Technical University of Cluj-Napoca, Department of Materials Science and Engineering, 103–105 Muncii Avenue, 400641 Cluj-Napoca, Romania

and octahedral. Among the spinel ferrites, nickel ferrite – $NiFe_2O_4$ is one of the most studied [11–16]. In the nickel ferrite structure the Ni^{2+} cations are distributed in octahedral sites and the Fe^{3+} cations are equally distributed between the tetrahedral and octahedral sites [10]. The spinel ferrites for common applications are generally obtained by solid state reaction at high temperature but, the use of the other synthesis methods has an increasing trend. The ferrites can be obtained as well by other methods such as: co-precipitation [1], sol-gel [2] or mechanosynthesis [11–13]. The properties of the nickel ferrite can be tailored by synthesis route or by adjusting its chemical composition. A classical way to adjust characteristics by modifying the chemical composition is to add other Me^{2+} cations, thus leading to $Ni_{1-x}Me_xFe_2O_4$ – nickel mixed ferrite [10, 13]. Another way is to introduce small amount of rare earth dopant cations. The electro-magnetic characterises of the ferrites can be improved by adding small amount of La^{3+}, Sm^{3+}, Y^{3+}, Dy^{3+} or Gd^{3+} cations [1, 6, 17–19].

The paper presents results concerning the influence of La^{3+} cations on the structural, morphological and thermal characteristics of simple nickel ferrite – $NiFe_2O_4$ using as precursors nickel and iron oxides and lanthanum hydroxide.

2. EXPERIMENTAL DETAILS

Nickel oxide – NiO (Alfa Aesar), iron oxide – Fe_2O_3 (Alfa Aesar) and lanthanum hydroxide – $La(OH)_3$ (Loba-Chemie Wien Fischamend) have been used as starting materials. All the powders have purity more than 90% and the particles size less than 40 μm. In order to obtain lanthanum doped nickel ferrite in the equimolar mixture of NiO and Fe_2O_3 an amount x of $La(OH)_3$ was introduced. The x = 0, 1, 2, 3 and 5 and represents the percent of NiO substituted in the starting samples. In the manuscript, the samples will be referring as 1% La in the case of $x = 1$, 2% La in the case of $x = 2$ and so on. The La_2O_3 results after the dehydration of the lanthanum hydroxide at temperature lower that the one where the ferrite is forming by solid state reaction.

The stoichiometric mixtures of oxides and hydroxide have been homogenized and after that subjected to heat treatment. The heat treatment has been carried out in air atmosphere at 1 200°C for 8 hours in a LAC heating furnace model VP 10\17. A schematic diagram of heat treatment (HT) parameters used for producing of lanthanum doped nickel ferrite and an image of the as obtained powder are shown in Fig. 1.

The X-ray diffraction (XRD) have been performed by an INEL EQUINOX 3 000 diffractometer, with CoKα radiation ($\lambda = 1.7903$ Å). The scanned interval was 2 theta = 20–110°. The powder in-situ high temperature X-ray diffraction (HT-XRD) investigations have been performed in preliminary vacuum up to 1 200 °C, using an Anton Paar HTK1200N heating furnace mounted on the above mentioned diffractometer.

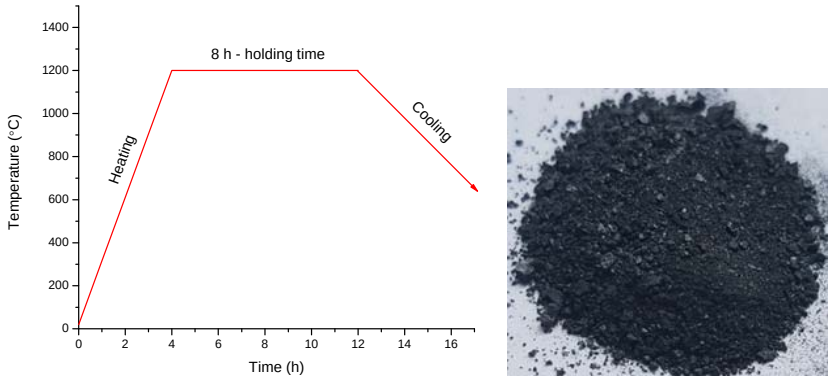

a) **b)**

Fig. 1 – a) Schematic diagram of heat treatment (HT) parameters
used for producing of lanthanum doped nickel ferrite; b) image of the as obtained powder.

The samples thermal stability was checked by differential scanning calorimetry (DSC) by a Setaram Labsys apparatus under argon flux. The DSC measurements were recorded up to 1 200 °C using a heating/cooling rate of 10 °C/min.

The powder morphology was analysed at different magnification levels by scanning electron microscopy (SEM) using a Jeol-JSM 5600 LV microscope. The local chemical homogeneity was investigated by X-ray Microanalysis using an Energy Dispersive Spectrometer (EDX) - Oxford Instruments, INCA 200 software.

3. RESULTS AND DISCUSSION

Figure 2 presents the X-ray diffraction patterns of the starting mixtures (0, 1, 2, 3 and 5 % La). In the same figure are presented the X-ray diffraction patterns of the $La(OH)_3$, NiO and Fe_2O_3. In the X-ray diffraction pattern of the lanthanum hydroxide ($La(OH)_3$) are identified the peaks characteristic of the hexagonal structure from P63/m space group according to JCPDS file no. 36–1481. In the case of NiO (bunsenite) diffraction pattern are noticed the peaks of the cubic structure from Fm-3m space group characteristic for this material (JCPDS file no. 47-1049). The hematite-Fe_2O_3 diffraction pattern presents its characteristic peaks, corresponding to the rhombohedral structure of R-3c space group (JCPDS file no. 33-0664). In starting samples (homogenized mixtures) the characteristic peaks for the iron oxide and nickel oxide are very well defined due to the well crystalized state and large amount of these phase.

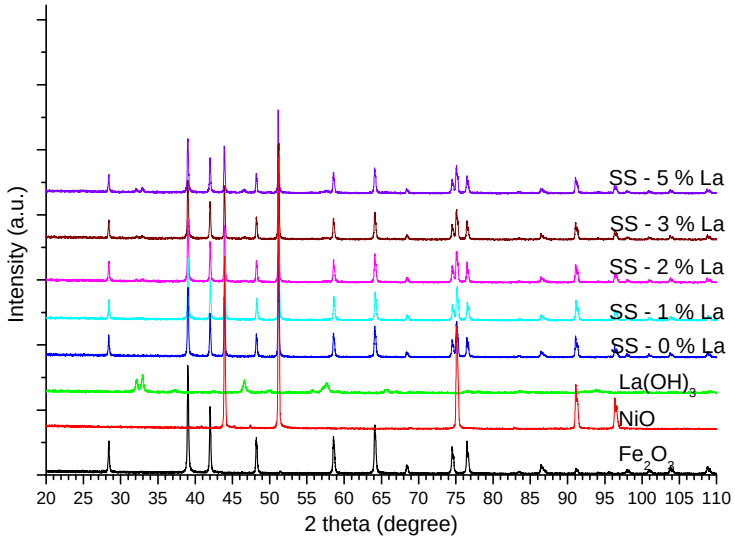

Fig. 2 – X-ray diffraction patterns of the starting mixtures (0, 1, 2, 3 and 5 % La), $La(OH)_3$, NiO and Fe_2O_3.

The characteristic peaks for the lanthanum hydroxide are not very well visible in the diffraction patterns due to the low amount of this phase in starting mixtures. The most intense peak of this phase is visible in the diffraction patterns independent on the amount in the starting mixtures (even in the case of 1% La) as can be seen in Fig. 3. In this figure is presented a detail of the X-ray diffraction patterns of the starting mixtures (0, 1, 2, 3 and 5 % La) and $La(OH)_3$ in the region where the most intense peaks of $La(OH)_3$, 2theta = 30–35°, is visible.

In Fig. 4 is presented the heating curve of the Differential Scanning Calorimetry (DSC) investigation for the starting mixture containing 5% La. In the DSC curve can be noticed a thermal event around at temperature of 390 °C. This endothermal event is assigned to the dehydration of the lanthanum hydroxide and the transformation of this after dehydration in lanthanum oxide – La_2O_3 [20]. The dehydration of the lanthanum hydroxide occurs according to the following reaction:

$$2 \cdot La(OH)_3 \rightarrow La_2O_3 + 3 \cdot H_2O \quad (1)$$

Upon increasing the temperature up to 1 200 °C no other noticeably thermal event is observed. After 550 °C it is reasonable to assume that the phases present in the homogenised mixture start to react leading to the formation of new phases. In order to check the presence of the phases formed upon heating X-ray diffraction have been performed to the sample heated in DSC furnace up to 1 200 °C.

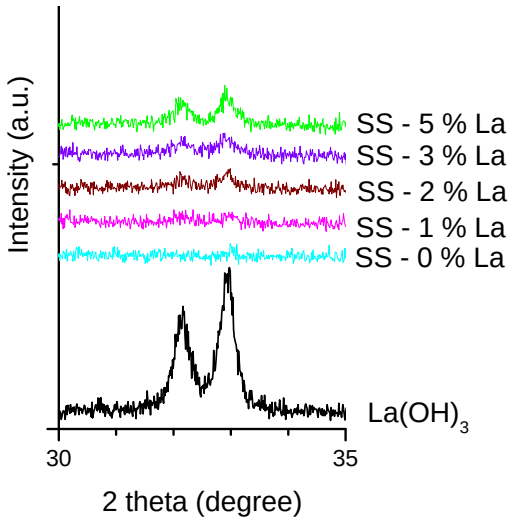

Fig. 3 – Detail of the X-ray diffraction patterns of the starting mixtures (0, 1, 2, 3 and 5 % La) and $La(OH)_3$ in the region of the most intense peaks of $La(OH)_3$.

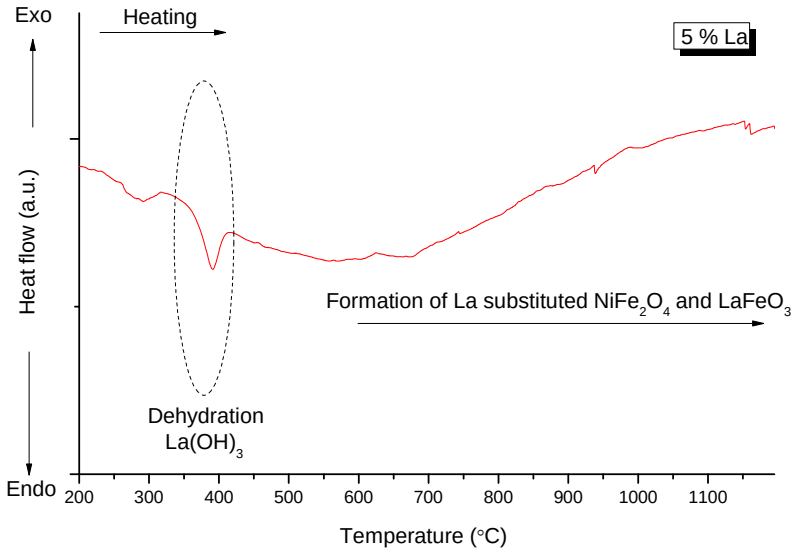

Fig. 4 – Heating curve of the Differential Scanning Calorimetry (DSC) investigation of the starting mixture containing 5% La.

In Fig. 5 is presented X-ray diffraction pattern of the sample containing 3% La after DSC at 1 200 °C in argon. Alongside of this pattern is presented also the X-ray diffraction pattern of the sample containing 5% La after XRD-HT at

1 200 °C in preliminary vacuum. Indeed, after heating in DSC the phases present in the starting mixture react leading to the formation of two new phases: a spinel ferrite cubic structure and iron lanthanum oxide orthorhombic structure. The spinel ferrite cubic structure has been indexed according to the JCPDS file no. 10-0325, trevorite ($NiFe_2O_4$), Fd-3m space group. The iron lanthanum oxide orthorhombic structure, $LaFeO_3$ (orthoferrite), has been indexed according to JCPDS file no. 37-1493, Pn*a space group.

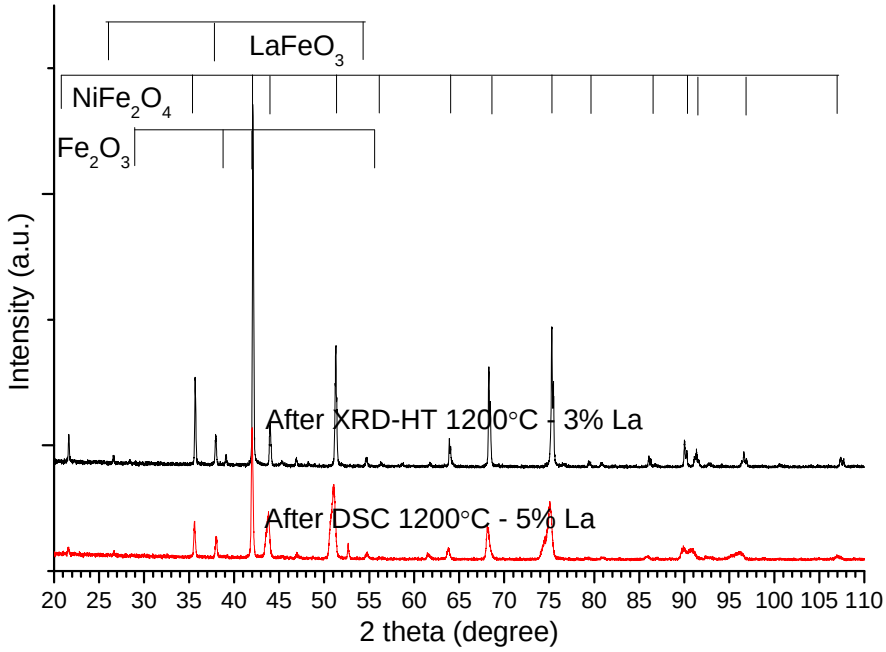

Fig. 5 – X-ray diffraction patterns of the sample containing 3% La after DSC at 1 200 °C in argon and sample containing 5% La after XRD-HT at 1200 °C in preliminary vacuum.

In the X-ray diffraction pattern of the sample containing 5% La heated in the X-ray diffractometer furnace in preliminary vacuum at 1 200 °C can be also observed the diffraction peaks of the same phases observed after DSC at 1 200 °C in argon (cubic spinel and orthoferrite) – Fig. 5. In addition, in this diffraction pattern can be observed the diffraction peaks of a hematite phase.

X-ray diffraction patterns of the samples heat treated (HT) at 1 200 °C for 8 h in air and doped with 0, 1, 2, 3 and 5 % La are presented in the Fig. 6. For reference are given the X-ray diffraction patterns of the $La(OH)_3$, NiO and Fe_2O_3. After this heat treatment, it can be observed that, independent on the amount of lanthanum introduced in the starting mixtures, there is no unreacted precursors ($La(OH)_3$, NiO or Fe_2O_3). In the case of the sample with 0% of lanthanum (undoped sample) in the diffraction pattern are identified only the peaks

corresponding to the cubic spinel structure of $NiFe_2O_4$. Thus, indicating a complete reaction during this heat treatment between NiO and Fe_2O_3 according to the following reaction:

$$NiO+Fe_2O_3 \rightarrow NiFe_2O_4 \quad (2)$$

In the case of the samples in which in the starting mixture an amount of lanthanum hydroxide has been introduced, beside spinel structure are observed the peaks corresponding to the lanthanum orthoferrite, $LaFeO_3$. Thus, indicating that during the heat treatment a reaction between the dehydrated lanthanum hydroxide and hematite occurs as follow:

$$La_2O_3+Fe_2O_3 \rightarrow 2\cdot LaFeO_3 \quad (3)$$

Another reaction that is possible during the heat treatment is the reaction of the nickel oxide with iron oxide and dehydrated lanthanum hydroxide and the formation of the lanthanum doped nickel ferrite. Such type of reaction can occur according to the following general reaction:

$$2\cdot NiO+ \delta\cdot La_2O_3+(2-\delta)\cdot Fe_2O_3 \rightarrow 2\cdot NiFe_{2-\delta}La_\delta O_4 \quad (4)$$

Due to the large volume of the lanthanum cations (La^{3+}) the presence in the cubic spinel structure of the nickel ferrite is limited [1–3]. This was indicated by the X-ray diffraction investigation. Indeed, it can be observed that even for a small amount of dopant element, 1% La, in the diffraction pattern are present the peaks of $LaFeO_3$. This means that less than 1% of lanthanum is present in the cubic spinel structure of the nickel ferrite. The lanthanum ion (La^{3+}) has a larger ionic radius as compared to Fe^{3+} cations radius (1.05 Å as compared to 0.67 Å [3]) this being one of the explanations of limited solubility of the lanthanum cations in the spinel structure. Taken into account that the nickel ferrite is an inverse spinel ferrite with the half of the Fe^{3+} cations in the tetrahedral site and half of the Fe^{3+} cations in the octahedral site alongside of the Ni^{2+} cations at a first glass it can be assumed that the La^{3+} can substitute Fe^{3+} cations from both sites. Due to the large radius of the La^{3+} cations it has preference for the octahedral sites [1, 2]. Also, it has been reported that the lanthanum cations can occupy interstices in the spinel cubic structure due to the large energy for activation of La^{3+} cations to enter in octahedral sites as compared to Fe^{3+} cations because the bond energy of La–O is stronger than that of Fe–O [1].

Upon increasing the amount of lanthanum in the samples the amount of the orthoferrite increases accordingly. The intensity of the diffraction peaks of the orthoferrite is increasing upon increasing the amount of lanthanum as compared to the intensity of the spinel ferrite peaks. According to the literature the amount of lanthanum that does not enter in the cubic spinel structure will form the orthoferrite secondary phase in the grain boundary of the cubic spinel ferrite [3].

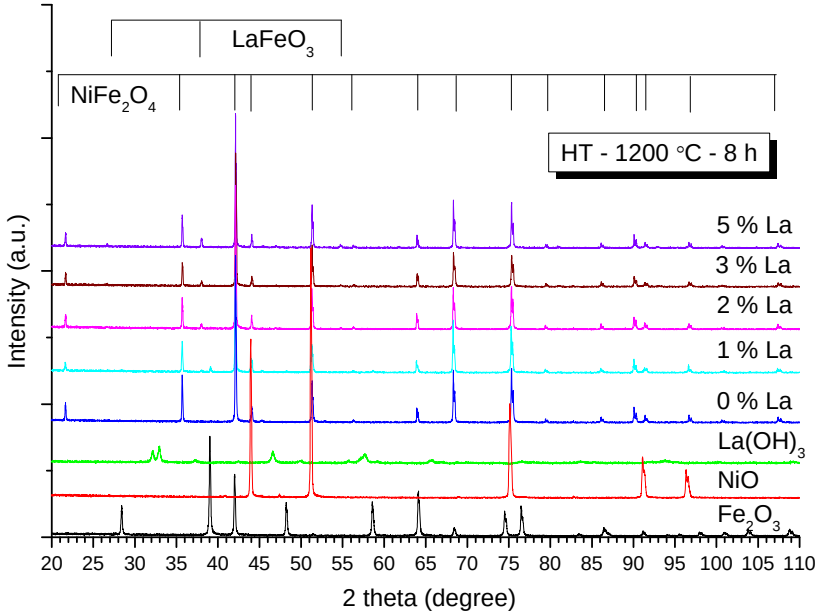

Fig. 6 – X-ray diffraction patterns of the samples heat treated (HT) at 1 200 °C for 8 h in air. For reference are given the X-ray diffraction patterns of the $La(OH)_3$, NiO and Fe_2O_3.

Scanning Electron Microscopy (SEM) images in Secondary Electron Image (SEI) mode of the samples containing 0, 3 and 5 % of La at a magnification of 1,000 and respectively 5,000× are shown in Fig. 7. It can be observed that the morphology of the sample is changing upon increasing the amount of lanthanum in the samples. The size and the shape of the grains differ when the amount of lanthanum differs in the samples. In the case of the doped samples it can be remarked that the porosity is diminishing upon increasing the dopant element amount.

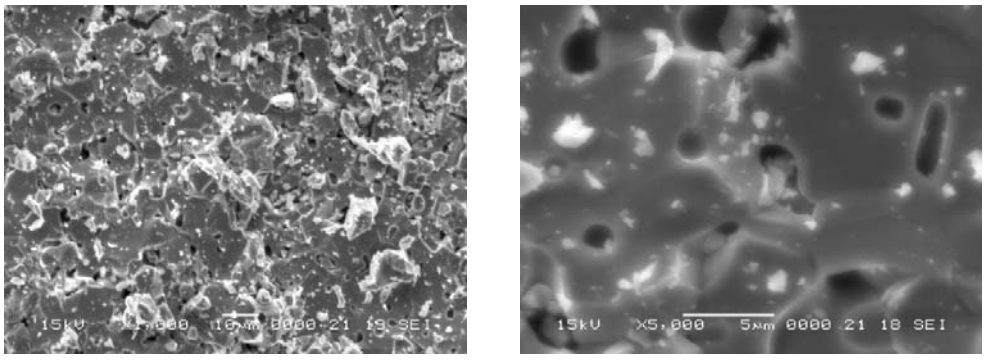

0 % La

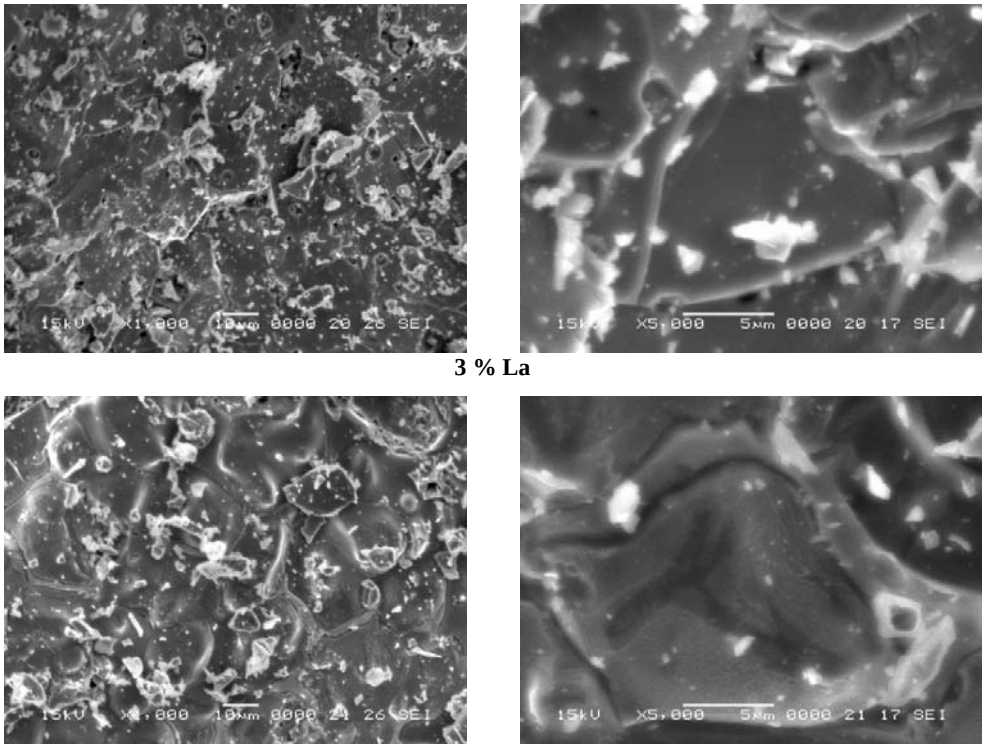

Fig. 7 – Scanning Electron Microscopy (SEM) images in Secondary Electron Image (SEI) mode of the samples containing 0, 3 and 5 % of La at a magnification of 1,000 and respectively 5,000×.

The large particles consist in large grains welded together which have some pores depending on dopant element concentration. It has been reported that in the doping of spinel ferrite with rare earth limit the grains growth [1, 2].

Distribution maps of Fe, Ni and O (EDX analysis) for the sample containing 0% La after heat treatment at 1 200 °C for 8h is shown in the Fig. 8. The chemical elements Fe, Ni and O are uniformly distributed in the investigated area. The lack of these chemical elements can be remarked in the pores zones.

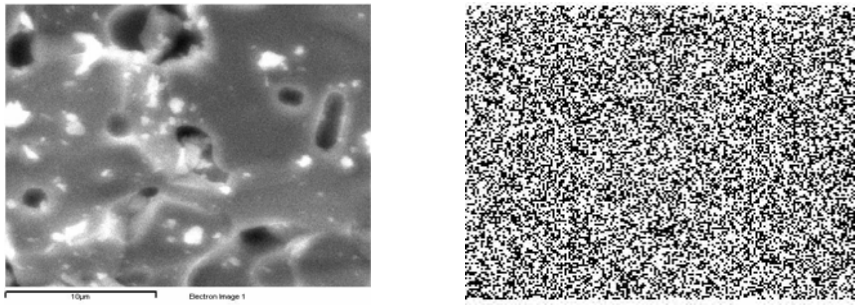

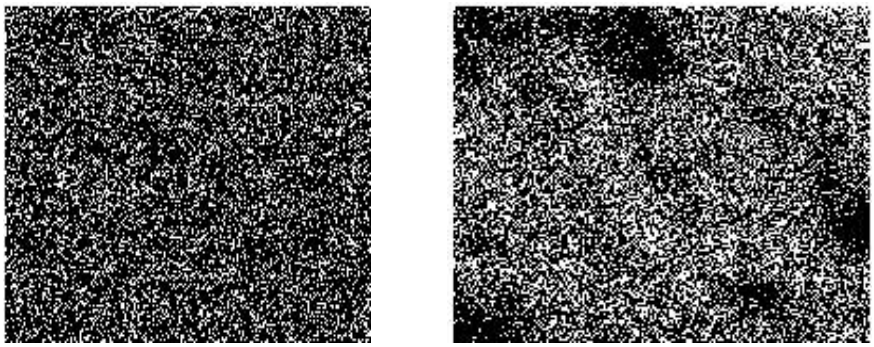

Nickel **Oxygen**

Fig. 8 – Distribution maps of chemical elements (EDX analysis) for the sample containing 0% La after heat treatment at 1 200 °C for 8 h.

In Fig. 9 are presented the Energy Dispersive X-ray Spectrometry (EDX) for the sample containing 5% La after heat treatment at 1 200 °C for 8 h. The distribution of the chemical elements, Fe, Ni, La and O is not uniform. It can be observed that in the investigated area it is a zone which follow the contour of the main grain and in which Fe, La and Ni have different concentrations as compared to the rest of the investigated area. In this zone (contour zone) the Ni it is almost inexistent, the Fe present low concentration as compared to the rest of the investigated area. In the same time, it can be observed a pronounced presence of the lanthanum as compared to the rest of the investigated area where the La presence is very low. The contour zone in which the Ni is not present and Fe has is less present and the La is present in large amount is associated with the $LaFeO_3$ chemical compound. The rest of the investigated area is associated with the presence of the cubic spinel phase of the lanthanum doped nickel ferrite. The lanthanum low quantity presence in this zone suggests the presence of the La^{3+} cations in the cubic spinel structure of the nickel ferrite.

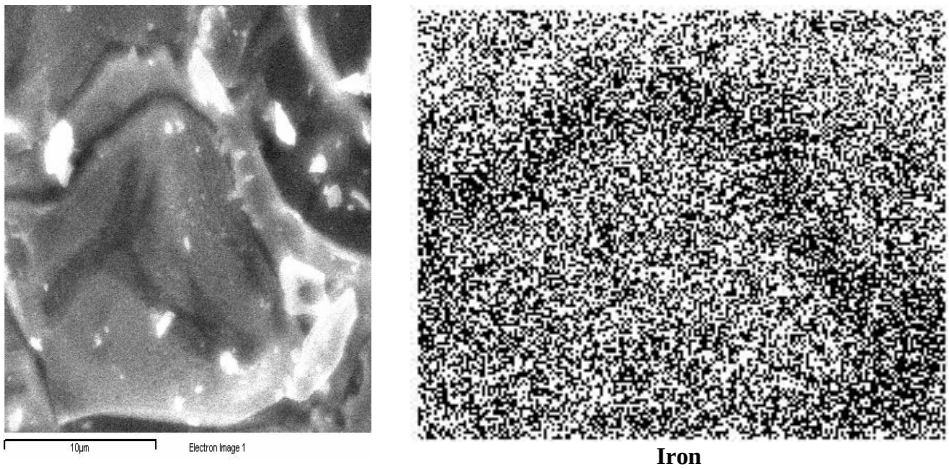

Iron

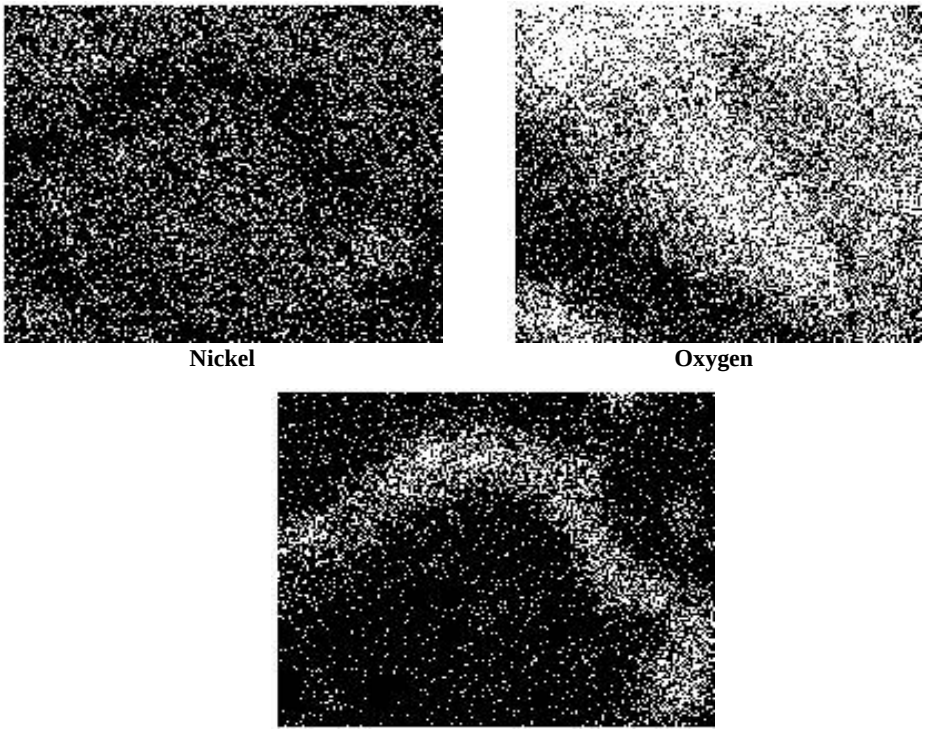

Fig. 9 – Distribution maps of the chemical elements (EDX analysis)
for the sample containing 5% La after heat treatment at 1 200 °C for 8 h.

These results are in good agreement with X-ray diffraction investigation and the earlier reported results concerning the doping of the cubic spinel ferrites.

4. CONCLUSIONS

The lanthanum doped nickel ferrite has been successfully synthesised by solid state reaction using as starting materials NiO, Fe_2O_3 and $La(OH_3)$. The amount of the chosen doping element that enter in the cubic spinel structure is less than 1 % – related to 100 % of the one atom of Ni from the chemical formula of nickel ferrite – $NiFe_2O_4$. The extra amount of the lanthanum from the samples leads to the formation of a secondary phase of $LaFeO_3$ type – orthoferrite. The secondary phase in the samples is situated at the grains boundary of the cubic spinel phase, following the contour of the grains. The presence of the lanthanum dopant element in the cubic spinel structure has been suggested by combining X-ray diffraction with the EDX microanalysis.

Received on October 4, 2017

REFERENCES

1. MENG, Y.Y., LIU, Z.W., DAI, H.C., YU, H.Y., ZENG, D.C., SHUKLA, S., RAMANUJAN, R.V., *Structure and magnetic properties of $Mn(Zn)Fe_{2-x}RE_xO_4$ ferrite nano-powders synthesized by co-precipitation and refluxing method*, Powder Technology, **229**, pp. 270–275, 2012.
2. ZHOU, X., JIANG, J., LI, L., XU, F., *Preparation and magnetic properties of La-substituted Zn-Cu-Cr ferrites via a rheological phase reaction method*, J. Magn. Magn. Mater., **314**, *1*, pp. 7–10, 2007.
3. CHAUDHARI, V., SHIRSATH, S.E., MANE, M.L., KADAM, R.H., SHELKE, S.B., MANE, D.R., *Crystallographic, magnetic and electrical properties of $Ni_{0.5}Cu_{0.25}Zn0_{.25}La_xFe_{2x}O_4$ nanoparticles fabricated by sol-gel method*, J. Alloys Compd., **549**, pp. 213–220, 2013.
4. REN, X., XU, G., *Electromagnetic and microwave absorbing properties of NiCoZn-ferrites doped with La^{3+}*, Journal of Magnetism and Magnetic Materials, **354**, pp. 44–48, 2014.
5. YADAV, N., KUMAR, A., RANA, P.S., RANA, D.S., ARORA, M., PANT, R.P., *Finite size effect on Sm^{3+} doped $Mn_{0.5}Zn_{0.5}Sm_xFe_{2-x}O_4$ ($0 \leq x \leq 0.5$) ferrite nanoparticles*, Ceramics International, **41**, *7*, pp. 8623–8629, 2015.
6. LIU, Z., PENG, Z., LV, C., FU, X., *Doping effect of Sm^{3+} on magnetic and dielectric properties of Ni-Zn ferrites,* Ceramics International, **43**, *1* (part B), pp. 1449–1454, 2017.
7. JACOBO, S.E., BERCOFF, P.G., *Structural and electromagnetic properties of yttrium-substituted Ni-Zn ferrites*, Ceramics International, **42**, *6*, pp. 7664–7668, 2016.
8. SNELLING, E.C., *Soft Ferrites (Properties and Applications)*, Iliffe Books Ltd, London, UK, 1969.
9. GOLDMAN, A., *Modern Ferrite Technology*, 2nd Ed., Springer Science-Business Media, USA, 2006.
10. CULLITY, B.D., GRAHAM, C.D., *Introduction to Magnetic Materials*, John Wiley&Sons, Inc., Hoboken, New Jersey, USA, 2009.
11. AZIZI, A., SADRNEZHAAD, S.K., *Effects of annealing on phase evolution, microstructure and magnetic properties of mechanically synthesized nickel-ferrite*, Ceramics International, **36**, *7*, pp. 2241–2245, 2010.
12. ŠEPELÁK, V., BAABE, D., MIENERT, D., SCHULTZE, D., KRUMEICH, F., LITTERST, F.J., BECKER, K.D., *Evolution of structure and magnetic properties with annealing temperature in nanoscale high-energy-milled nickel ferrite*, J. Magn. Magn. Mater., **257**, pp. 377–386, 2003.
13. MARINCA, T.F., CHICINAŞ, I., ISNARD, O., NEAMŢU, B.V., *Nanocrystalline/nanosized manganese substituted nickel ferrites – $Ni_{1-x}Mn_xFe_2O_4$ obtained by ceramic-mechanical milling route*, Ceramics International, **42**, *4*, pp. 4754–4763, 2016.
14. YANG, H., ZHANG, X., AO, W., QIU, G., *Formation of $NiFe_2O_4$ nanoparticles by mechanochemical reaction*, Mater. Res. Bull., **39**, *6*, pp. 833–837, 2004.
15. MARINCA, T.F., CHICINAŞ, I., ISNARD, O., POP, V., POPA, F., *Synthesis, structural and magnetic characterisation of nanocrystalline nickel ferrite – $NiFe_2O_4$ obtained by reactive milling*, J. Alloys Compd., **509**, pp. 7931–7936, 2011.
16. CHINNASAMY, C.N., NARAYANASAMY, A., PONPANDIAN, N., CHATTOPADHYAY, K., SHINODA, K., JEYADEVAN, B., TOHJI, K., NAKATSUKA, K., FURUBAYASHI, T., NAKATANI, I., *Mixed spinel structure in nanocrystalline $NiFe_2O_4$*, Physical Review B, **63**, *18*, no. 184108, 2001.
17. WANG, Y., WU, X., ZHANG, W., CHEN, W., *Synthesis and electromagnetic properties of La-doped Ni-Zn ferrites*, J. Magn. Magn. Mater., **398**, pp. 90–95, 2016.
18. STERGIOU, C., *Magnetic, dielectric and microwave absorption properties of rare earth doped Ni-Co and Ni-Co-Zn spinel ferrites*, J. Magn. Magn. Mater., **426**, pp. 629–635, 2017.
19. INBANATHAN, S.S.R., VAITHYANATHAN, V., CHELVANE, J.A., MARKANDEYULU, G., BHARATHI, K.K., *Mössbauer studies and enhanced electrical properties of R (R=Sm, Gd and Dy) doped Ni ferrite*, J. Magn. Magn. Mater., **353**, pp. 41–46, 2014.
20. FÜGLEIN, E., WALTER, D., T*hermal behavior of lanthanum hydroxide in the dependency of pressure*, Z. Anorg. Allg. Chem., **632**, pp. 2154–2157, 2006.